ORIGINAL PAPER

Effect of La–Zn Substitution on the Structure and Magnetic Properties of Low Temperature Co-Fired M-Type Barium Ferrite

Jie Li · Huaiwu Zhang · Yuanxun Li · Qiang Li · Guoliang Yu

Abstract $Ba(LaZn)_x Fe_{12-2x} O_{19}$ $(0 \leq x \leq 0.5)$ powders with Bi_2O_3 as an additive was synthesized by a sintered route at 900 °C or 950 °C. The structure and magnetic properties of La–Zn substituted M-type barium ferrites were also investigated. When $0 \leq x \leq 0.5$, only one crystal phase existed in the sample, and the morphology of the grains were shown to be gradually irregular. The little amount of La^{3+} ions and Zn^{2+} ions changed the equilibrium of Fe^{2+} and Fe^{3+} at the 2a site, which increased the $Fe^{3+}–O–Fe^{2+}$ superexchange interaction strength, and the saturation magnetization (Ms) of the samples was also improved. Meanwhile, the substitution of La^{3+} and Zn^{2+} ions and the grains' size bought great effects on the magnetocrystalline anisotropy field. As a result, with sintering at 950 °C for 6 h, the max Ms value of the samples with $x = 0.1$ was 67.26 emu/g, and the minimum coercivity (H_c) value was 1718.89 Oe with $x = 0.3$, respectively.

1 Introduction

M-type barium ferrite has been widely applied in permanent magnets and perpendicular high density for its good magnetic properties and low price to produce [1, 2]. Meanwhile, the next generation magnetic microwave devices required the barium ferrite with a high remanent magnetization. The applications of recording media required a higher

J. Li (✉) · H. Zhang · Y. Li · Q. Li · G. Yu
State Key Laboratory of Electronic Thin Films and Integrated Devices, University of Electronic Science and Technology of China, Chengdu 610054, China
e-mail: lijie8594@gmail.com

standard for barium ferrite materials [3, 4]. In the present study, three important methods have been employed to adapt the requirement of low temperature cofired ferrites technology and produce devices with a multilayer process: lowering the sintered temperature [5, 6], increasing the value of saturation magnetization [7], and changing the magnetocrystalline anisotropy constant [8]. As for improving the magnetic properties of barium ferrite, many works focused on the synthesis of ferrite [9–11], such as optimizing the sintering process [12–14], and the substitution of suitable ions, [15] etc. Among these methods, the ions' substitution is considered an effective approach to change the properties of BaM ferrites. The substitution of Ba^{2+}- or Fe^{3+}-sites has been extensively investigated in recent years, for example, La^{3+}, Gd^{3+}, $Sm^{4+}–Zn^{2+}$, $Cr^{4+}–Zn^{2+}$, $La^{3+}–Zn^{2+}$, and $Sn^{4+}–Mg^{2+}$ [16–23]. Low coercivity and high saturation magnetization values were synchronously required for use in recording media applications; therefore, reduction in the coercivity along with the increase in the saturation magnetization was a new goal in preparing barium ferrites.

Recently, with the development of low temperature cofired ceramic (LTCC) technology, the low temperature cofired magnetic materials have drawn more concerns. Barium ferrites keep excellent properties at a low sintering temperature, which is the aim of the investigation. The influence of the La–Zn substituted barium ferrites have been reported, but almost all were $Ba_{1-x}(LaZn)_x Fe_{12-x} O_{19}$ materials. In this work, the $Ba(LaZn)_x Fe_{12-2x} O_{19}$ ferrite powders were synthesized with the solid state method and sintered with a low temperature, and the structure and magnetic properties of the ferrites were discussed.

Table 1 Variation of hexagonal lattice parameters, cell volume and density with La–Zn substitution

x	a (Å)	c (Å)	V (Å^3)	Density (g/cm^3)
0.0	5.8865(2)	23.1843(2)	695.73	5.3046
0.1	5.8907(2)	23.1833(3)	696.72	5.2980
0.2	5.8923(4)	23.1849(5)	697.04	5.2948
0.3	5.8946(3)	23.1850(2)	697.65	5.2909
0.4	5.8937(3)	23.1762(3)	697.19	5.2943
0.5	5.8941(2)	23.1804(4)	697.35	5.2912
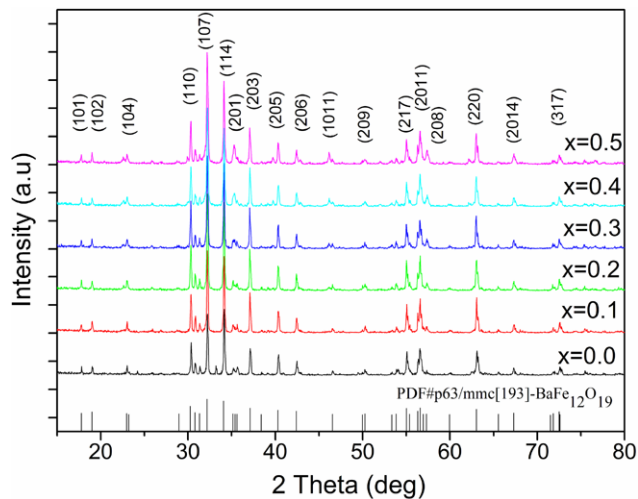
Fig. 1 X-ray patterns of the Ba(LaZn)$_x$Fe$_{12-2x}$O$_{19}$ samples sintered at 950 °C

2 Experiment

Powders of Ba(LaZn)$_x$Fe$_{12-2x}$O$_{19}$ with $0 \leq x \leq 0.5$ were prepared using the solid state method. BaCO$_3$, Fe$_2$O$_3$, La$_2$O$_3$, and ZnO, as the raw materials, were mixed by the molar ratio and ball milled for 24 h and presintered in air at 950 °C. Then the powders were mixed with 2.5 wt% Bi$_2$O$_3$ and milled for 18 h, dried, and sintered at 900 °C and 950 °C in the air.

The phase compositions of the samples were investigated by an X-ray diffractometer (XRD, DX-2700, Haoyuan Co.) with Cu K$_\alpha$ radiation; the lattice parameters and cell volume, and the density of the samples were calculated based on XRD data. The micrographs of the samples were carried out using a scanning electron microscope (SEM, JEOL, JSM-6490). The magnetic properties of the samples were measured using a vibrating sample magnetometer (VSM, MODEL BHV-525).

3 Results and Discussion

The XRD patterns of Ba(LaZn)$_x$Fe$_{12-2x}$O$_{19}$ ferrites sintered at 950 °C with different x contents are shown in Fig. 1.

It can be seen that with the increased x content, all the samples show the typical peaks of the pure hexagonal ferrite phase (P63/mmc (194)-M-type BaFe$_{12}$O$_{19}$). The lattice parameters, cell volume, and the density of the samples sintered at 950 °C were listed in Table 1. When $x \leq 0.3$, the lattice parameters, a and c reach the maximum value with x increasing. The slight changes in the lattice constant were attributed to the ionic radius of La^{3+} (1.061 Å) and Zn^{2+} (0.74 Å), which are larger than that of Fe^{3+} (0.645 Å). It could be probable that the La^{3+} and Zn^{2+} ions entered the crystalline lattice and changed the lattice properties of the samples. Thus, the decreased lattice constant showed that the La–Zn ions substitution was accomplished. When $x \geq 0.3$, superfluous La–Zn ions existed between the crystalline, which resulted in the decrease of the lattice parameters.

The micrographs of fractured cross-sections of the samples were characterized by SEM and shown in Fig. 2. The SEM of the sample showed that well-formed hexagonal grains and the mean particle sizes were 1 μm. With the increase of La–Zn, the shape of samples became irregular gradually and some small particles appeared. The difference between the samples could be the content of La–Zn substitution and the agglomeration of grains. The ferrites formation reaction was promoted by the La^{3+} and Zn^{2+} ions, which was in agreement with other researches [24].

The changes of the saturation magnetization (Ms) and coercivity (H_c) of the samples with the La–Zn substitution were shown in Fig. 3. Variations in Ms and H_c for the samples were shown in Fig. 4. With different sintering temperatures, the Ms of the samples increased with x contents and reached 54.54 emu/g and 53.68 emu/g at $x = 0.1$, and then decreased gradually. Meanwhile, the H_c first decreased to the minimum value of 1969.07 Oe and 1635.54 Oe at $x = 0.3$, which revealed the samples exhibit a typical soft magnetic characteristic trend with a specific saturation magnetization. However, H_c increased when $x \geq 0.2$.

The natural magnetic properties of the ferrites were impacted directly by the chemical composition. In the basic structure of M-type barium ferrites, Fe^{3+} ions occupy five different interstitial sites: tetrahedral 4f$_1$ ($\downarrow$), bipyramidal 2b ($\uparrow$), and three octahedral sites 12 K ($\uparrow$), 4f$_2$ ($\downarrow$), and 2a ($\uparrow$). When La^{3+} and Zn^{2+} substitute Fe^{3+} ions, the La^{3+} ions

Fig. 2 SEM micrographs of the samples sintered at 950 °C

a. x=0.0

b. x=0.1

c. x=0.2

d. x=0.3

e. x=0.4

f. x=0.6
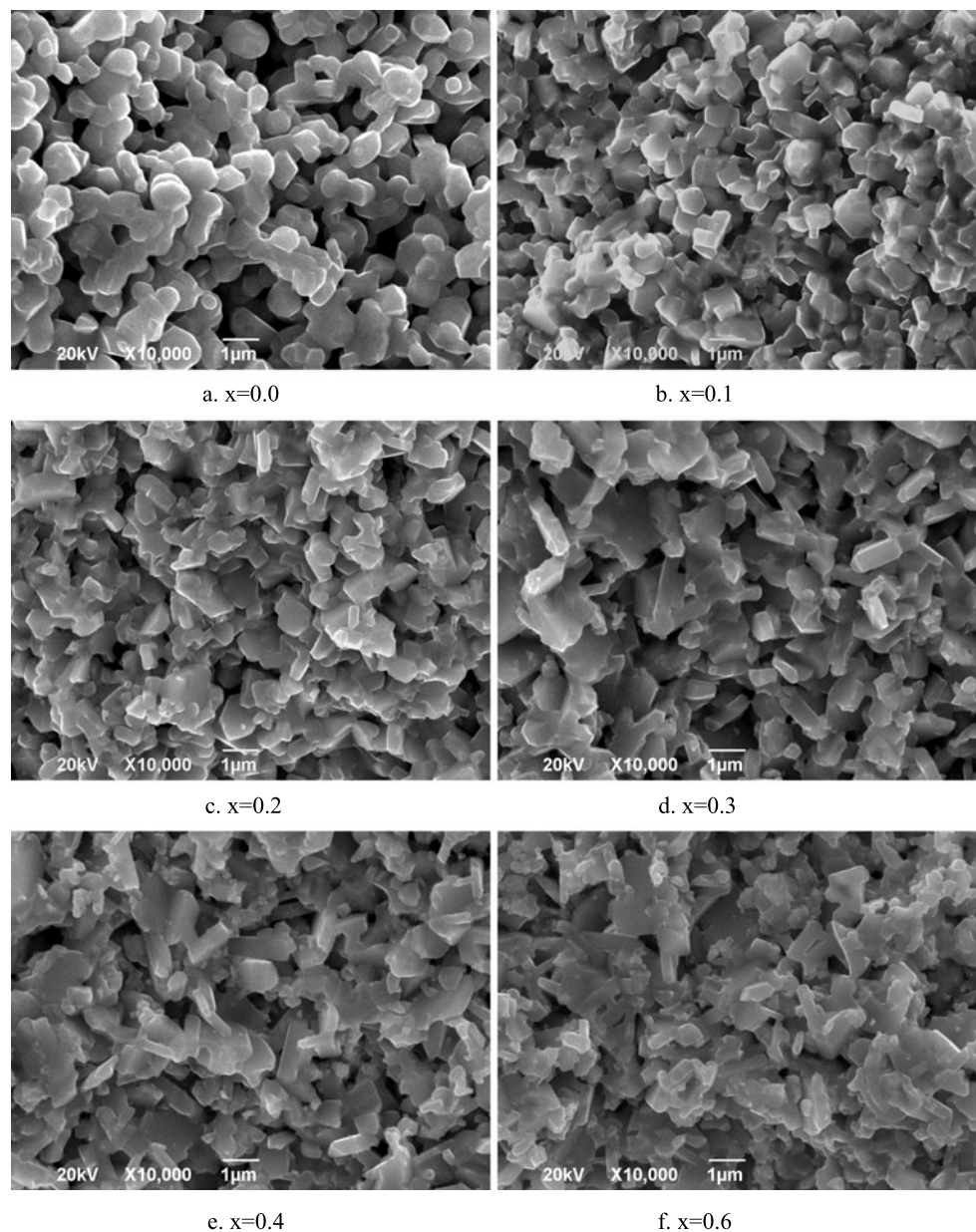
preferentially substitute the Fe^{3+} ions at the 2a or $4f_2$ sites, and nearly all Zn^{2+} ions substitute Fe^{3+} ions at the $4f_1$ site, which results in a valence change of Fe^{3+} to Fe^{2+} at the 2a site. This position will increase the number of Fe^{3+} ions in spin-up sites compared with spin-down sites, and as a result, it increases the saturation magnetization of the samples with the increase of x ($x \leq 0.1$). However, when $x > 0.1$, the saturation magnetization decreased because of superfluous nonmagnetic Zn^{2+} ions.

According to the Stoner–Wohlfarth model theory, the magnetictocrystalline anisotropy energy (E_A) of the sample is approximated by

$$E_A = KV \sin^2 \theta$$

where K is anisotropy constant, V is the volume of crystal, and θ is the angle between the easy axis and the direc-

tion of filed-induced magnetization. H_c is closely related to E_A, which is proportional to the product K and V, and H_c is related to the grain size. The first decrease of coercivity H_c may be due to the fact that the decrease of the magnetocrystalline anisotropy field results from the substitution of nonmagnetic Zn^{2+} ions and the changes of the grains' size. When $x > 0.3$, the increase of H_c can be attributed to the enhancement of the magnetocrystalline anisotropy, which dues to too many Fe^{2+} ions locating on 2a site.

4 Conclusions

$Ba(LaZn)_x Fe_{12-2x} O_{19}$ ($0 \leq x \leq 0.5$) powders with Bi_2O_3 as an additive was synthesized by a sintered route at 900 °C
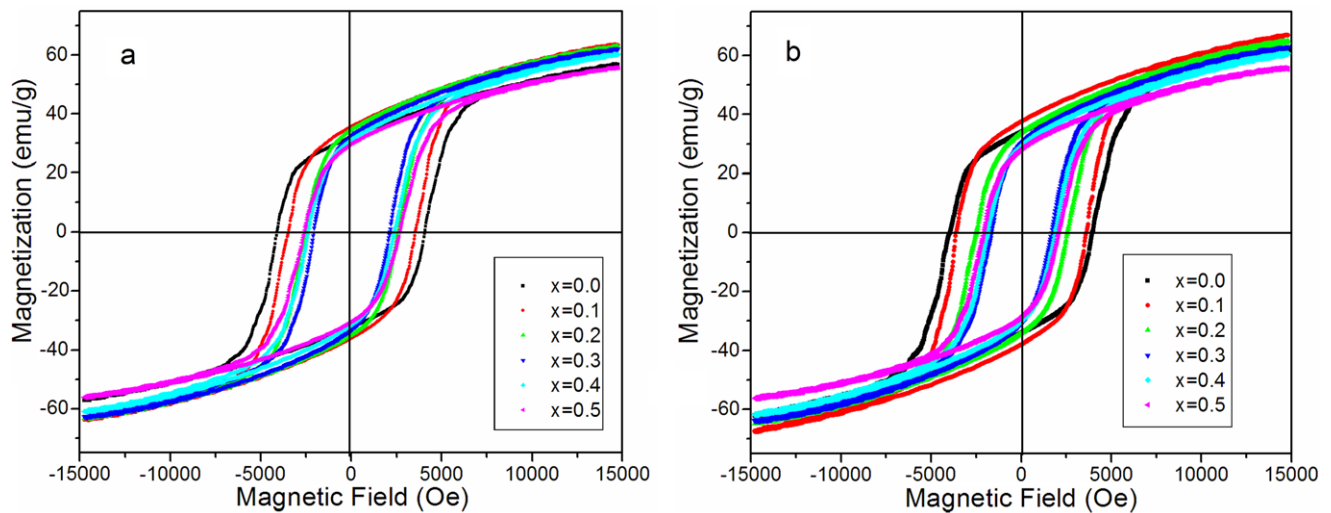
Fig. 3 M–H hysteresis loops of the samples with composition $0 \leq x \leq 0.5$ in $Ba(LaZn)_x Fe_{12-2x} O_{19}$ prepared by sintering at 900 °C (**a**) and 950 °C (**b**) in air
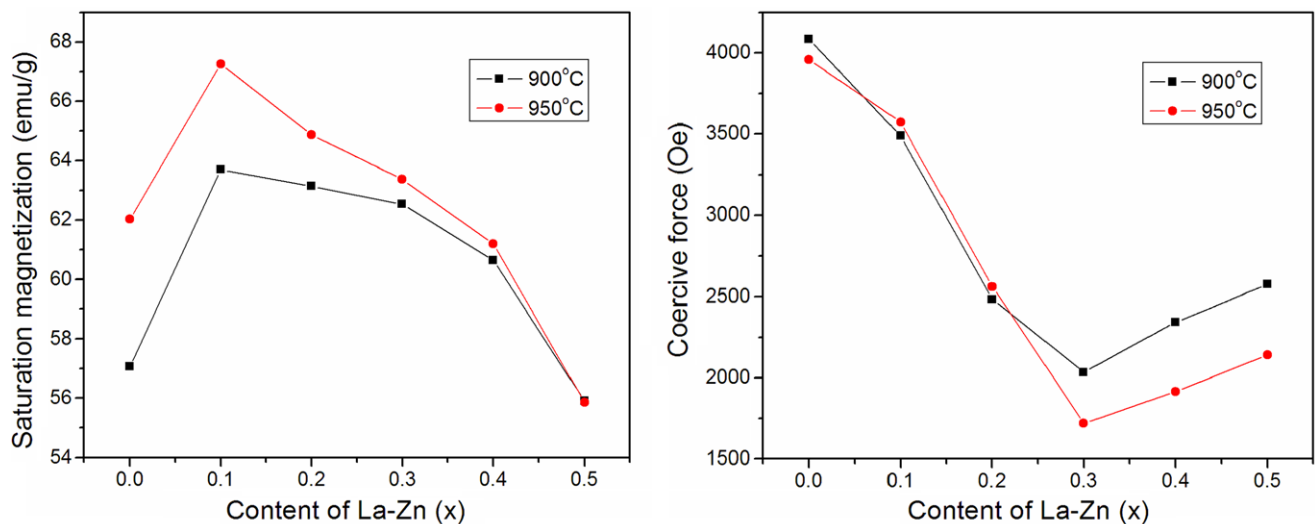
Fig. 4 Compositional dependences of the saturation magnetization and the coercive force

or 950 °C. When $0 \leq x \leq 0.5$, only one crystal phase existed in the sample, and the morphology of the grains were shown to be gradually irregular. The lattice parameters were adjusted by the content of the La–Zn substitution. The saturation magnetization increased at a low substitution content of $x = 0.1$ and decreased for $x > 0.2$. The coercivity decreased from $x = 0.0$ to $x = 0.3$, and then increased. The phenomenon was attributed to particle size, nonmagnetic impurity phases, and the site preference of the La–Zn substitution.

References

1. Kikuchi, T., Nakamura, T., Yamasaki, T., Nakanushi, M., Fujii, T., Takada, J., Ikeda, Y.: Magnetic properties of La-Co substituted M-type strontium hexaferrites prepared by polymerizable complex method. J. Magn. Magn. Mater. **322**, 2381–2385 (2010)
2. Zi, Z.F., Liu, Q.C., Dai, J.M., Sun, Y.P.: Effects of Ce-Co substitution on the magnetic properties of M-type barium hexaferrites. Solid State Commun. **152**, 894–897 (2012)
3. Harris, V.G., Chen, Z.H., Chen, Y.J., Yoon, S., Sakai, T., Gieler, A., Yang, A., He, Y.X.: Ba-hexaferrite films for next generation microwave devices. J. Appl. Phys. **99**, 08M911 (2006)

4. Sui, X.Y., Scherge, M., Kryder, M.H., Snyder, J.E., Harris, V.G., Koon, N.C.: Barium ferrite thin-film recording media. J. Magn. Magn. Mater. **155**, 132–139 (1996)

5. Rane, M.V., Bahadur, D., Kulkarni, S.D., Date, S.K.: Magnetic properties of NiZr substituted barium ferrite. J. Magn. Magn. Mater. **195**, L256–L260 (1999)

6. Dhage, V.N., Mane, M.L., Babrekar, M.K., Kale, C.M., Jadhav, K.M.: Influence of chromium substitution on structural and magnetic properties of $BaFe_{12}O_{19}$ powder prepared by sol-gel auto combustion method. J. Alloys Compd. **509**, 4394–4398 (2011)

7. Ashiq, M.N., Iqbal, M.J., Najam-ul-Haq, M., Gomez, P.H., Qureshi, A.M.: Synthesis, magnetic and dielectric properties of Er-Ni doped Sr-hexaferrite nanomaterials for applications in high density recording media and microwave devices. J. Magn. Magn. Mater. **324**, 15–19 (2012)

8. Kakizaki, K., Taguchi, H., Hiratsuka, N.: Magnetic properties of La-Co substituted barium ferrite thin films with large magnetic anisotropy. J. Magn. Magn. Mater. **272–275**, 2241–2243 (2004)

9. Gomez, E., Pane, S., Valles, E.: Magnetic composites CoNi-barium ferrite prepared by electrodeposition. Electrochem. Commun. **7**, 1225–1231 (2005)

10. Janasi, S.R., Emura, M., Landgraf, F.J.G., Rodrigues, D.: The effects of synthesis variables on the magnetic properties of coprecipitated barium ferrite powders. J. Magn. Magn. Mater. **238**, 168–172 (2002)

11. Harris, V.G., Geiler, A., Chen, Y.J., Yoon, S., Wu, M.Z., Yang, A., Chen, Z.H., He, P., Parimi, P.V., Zuo, X., Patton, C.E., Abe, M., Acher, O., Vittoria, C.: Recent advances in processing and applications of microwave ferrites. J. Magn. Magn. Mater. **321**, 2035–2047 (2009)

12. Chinnasamy, C.N., Sakai, T., Sivasubramanian, S., Yang, A.F., Vittoria, C., Harris, V.G.: Magnetic and microwave properties of basal-plane oriented $BaFe_{11}In_1O_{19}$ ferrite thick films processed by screen printing. J. Appl. Phys. **103**, 07F710 (2008)

13. Vincent, G.H.: Modern microwave ferrite. IEEE Trans. Magn. **48**(3), 1075–1104 (2012)

14. Bierlich, S., Topfer, J.: Low-temperature firing of substituted M-type hexagonal ferrites for multilayer inductors. IEEE Trans. Magn. **48**(4) (2012)

15. Haq, A., Anis-ur-Rehman, M.: Effect of Pb on structural and magnetic properties of Ba-hexaferrite. Physica B **407**, 822–826 (2012)

16. Li, C.J., Wang, B., Wang, J.N.: Magnetic and microwave absorbing properties of electrospun $Ba_{(1-x)}La_xFe_{12}O_{19}$ nanofibers. J. Magn. Magn. Mater. **324**, 1305–1311 (2012)

17. Sozeri, H., Kucuk, I., Ozkan, H.: Improvement in magnetic properties of La substituted $BaFe_{12}O_{19}$ particles prepared with an unusually low Fe/Ba molar ratio. J. Magn. Magn. Mater. **323**, 1799–1804 (2011)

18. Litsardakis, G., Manolakis, I., Derletis, C., Efthimiadis, K.G.: High coercivity Gd-substituted Ba hexaferrites, prepared by chemical coprecipitation. J. Appl. Phys. **103**, 07E501 (2008)

19. Han, Y.B., Sha, J., Sun, L.N., Tang, Q., Lu, Q.: Tailored magnetic properties of Sm(Zn) substituted nanocrystalline barium hexaferrites. J. Alloys Compd. **486**, 348–351 (2009)

20. Asghar, G., Anis-ur-Rehman, M.: Structural, dielectric and magnetic properties of Cr-Zn doped strontium hexa-ferrites for high frequency applications. J. Alloys Compd. **526**, 85–90 (2012)

21. Gruskova, A., Lipka, J., Papanova, M., Slama, J., Toth, I.: La-Zn substituted hexaferrites prepared by chemical method. Hyperfine Interact. **164**, 27–33 (2006)

22. Hua, Z.H., Li, S.Z., Han, Z.D., Wang, D.H., Lu, M., Zhong, W., Gu, B.X., Du, Y.W.: The effect of La-Zn substitution on the microstructure and magnetic properties of barium ferrites. Mater. Sci. Eng., A **448**, 326–329 (2007)

23. Davoodi, A., Hashemi, B.: Magnetic properties of Sn-Mg substituted strontium hexaferrite nanoparticles synthesized coprecipitation method. J. Alloys Compd. **509**, 5893–5896 (2011)

24. Singh, C., Bindra Narang, S., Hudiara, I.S., Bai, Y., Tabatabaei, F.: Static magnetic properties of Co and Ru substituted Ba-Sr ferrite. Mater. Res. Bull. **43**, 176–184 (2008)